2009 American Control Conference
Hyatt Regency Riverfront, St. Louis, MO, USA
June 10-12, 2009



# Real-Time Estimation of Roll Angle and CG Height for Active Rollover Prevention Applications

R. Rajamani [1], D. Piyabongkarn [2], V. Tsourapas [2] and J.Y. Lew [2]

*Abstract*— **Roll angle and height of the center of gravity are important variables that play a critical role in the calculation of real-time rollover index for a vehicle. The rollover index predicts the real-time propensity for rollover and is used in activation of rollover prevention systems such as differential braking based stability control systems. Sensors to measure roll angle are expensive. Sensors to estimate the c.g. height of a vehicle do not exist. While the height of the center-of-gravity does not change in real-time, it does change with the number of passengers and loading of the vehicle. This paper focuses on algorithms to estimate roll angle and c.g. height. The algorithms investigated include a sensor fusion algorithm that utilizes a low frequency tilt angle sensor and a gyroscope and a dynamic observer that utilizes only a lateral accelerometer and a gyroscope. The performance of the developed algorithms is investigated using simulations and experimental tests. Experimental data confirm that the developed algorithms perform reliably in a number of different maneuvers that include constant steering, ramp steering, double lane change and sine with dwell steering tests.**

## 1. INTRODUCTION

Vehicle rollovers account for a significant fraction of highway traffic fatalities. While only 3% of vehicle accidents result in rollovers, 33% of all fatalities have vehicle rollover as a contributing factor [8]. Hence there is significant research being conducted on development of active rollover prevention systems [1, 2, 3, 4, 5, 6, 7, 9, 11, 13, 14]. An active rollover prevention system typically utilizes differential braking to reduce the yaw rate of the vehicle and to slow down the vehicle speed. Both of these factors contribute to reducing the propensity of the vehicle to rollover.

An important challenge in the design of an active rollover prevention system is the calculation of the rollover index which indicates the likelihood of the vehicle to rollover and is used to trigger differential braking to prevent rollover. Accurate calculation of the rollover index is important in order to ensure that rollovers can be prevented in time while at the same ensuring that active rollover prevention is not triggered unnecessarily.

One method of defining the rollover index is based on the use of the real-time difference in vertical tire loads between left and right sides of the vehicle. Figure 1 shows a schematic of a vehicle with a sprung mass that undergoes roll motion. The difference between the vertical tire forces $F_{z\ell}$ and $F_{zr}$ caused by the roll motion of the vehicle is used to define the rollover index $R$ [7]:

$$R = \frac{F_{z\ell} - F_{zr}}{F_{z\ell} + F_{zr}} \tag{1}$$

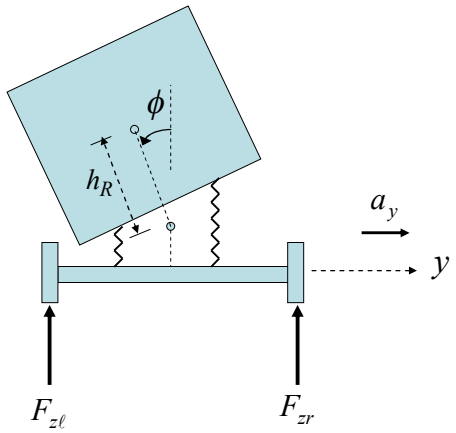


**Figure 1: Rollover index using lateral load transfer**

If we assume that the roll motion of the sprung mass is caused entirely by the lateral acceleration of the vehicle (ignoring road and other external inputs), then it can be shown that the rollover index of equation (1) can be represented as [9]

$$R = \frac{2h_R a_y \cos\phi + 2h_R \sin\phi}{\ell_w g \cos\phi} \tag{2}$$

where $h_R$ is the height of the center-of-gravity (c.g.) of the vehicle from the roll center of the sprung mass and $a_y$ is the lateral acceleration of the vehicle measured on the unsprung mass.

It should be noted that the rollover index of equation (2) needs measurement of lateral acceleration $a_y$, roll angle $\phi$ and knowledge of the height of the c.g. $h_R$. However, roll angle cannot be measured easily in a vehicle. Suspension deflection measurements on the left and right sides of the vehicle are required in order to calculate roll angle. Since suspension deflection sensors are expensive, real-time measurement of roll angle is typically not available on a passenger vehicle.

Hence the rollover index of equation (2) is typically approximated by

[1] **R. Rajamani is with the University of Minnesota, Minneapolis, MN 55455, Email: rajamani@me.umn.edu**

[2] **D. Piyabongkarn, V. Tsourapas and J. Y. Lew are with Eaton Corporation, Innovation Center, Eden Prairie, MN 55344, Email: NengPiyabongkarn@eaton.com, JaeYLew@eaton.com**

$$R_{approx} = \frac{2h_R a_y}{\ell_w g} \tag{3}$$

This paper focuses on the accurate estimation of roll angle and the estimation of height of the c.g. of the vehicle so as to enable implementation of the original rollover index calculation of equation (2).

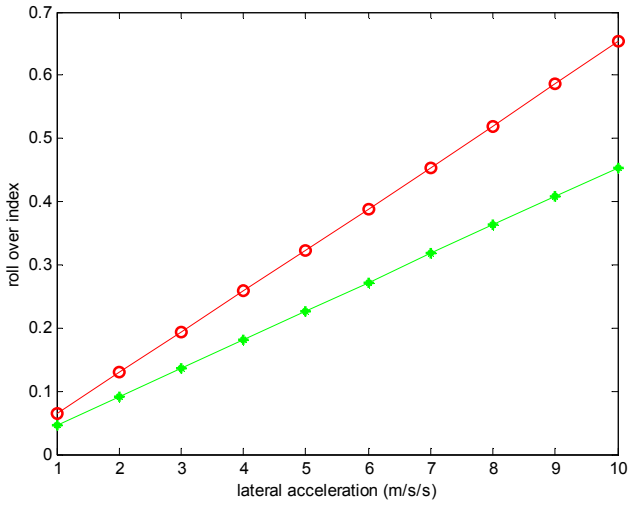


**Figure 2: Rollover indices $R$ (circles) and $R_{approx}$ (stars) as a function of lateral acceleration**

Figure 2 shows the original rollover index $R$ and its approximation $R_{approx}$ as a function of lateral acceleration during steady state cornering around a circular track for a Volvo XC 90 SUV. It can be seen that the difference between the two curves increases as lateral acceleration increases, resulting in higher error during tight cornering maneuvers. Further, the error increases with increase in height of the c.g. This motivates the need to estimate roll angle so as use a more accurate calculation of the rollover index.

It should be noted that the height of the c.g. is a constant parameter. However, it changes with change in the passenger and freight load on the vehicle. In the case of SUVs and military vehicles, the change in c.g. height can be very significant and as much as 100% of nominal height. This paper therefore also develops and evaluates an algorithm for real-time estimation of c.g. height.

## 2. KINEMATIC SENSOR FUSION

As a first step, consider the use of a gyroscope and a tilt angle sensor to estimate the roll angle of the vehicle. While the gyroscope can measure roll rate, the presence of a time-varying bias makes the direct estimation of roll angle by integration of the gyroscope signal impossible.

A tilt angle sensor consisting of the Crossbow CXTD02 inertial angle sensor can be used to supplement the gyroscope. The Crossbow tilt angle sensor consist of two-axis in-built accelerometers and signal processing algorithms that enable static tilt angle to be calculated from the accelerometer measurements. An example of an algorithm that can be used for this purpose can be found in [10].

Since the gyroscope can measure roll rate while the tilt angle sensor can measure static (or low frequency) roll angle, the signals from the two sensors can be combined to obtain good estimates of both roll angle and roll rate. The following kinematic fusion algorithm is suggested:

$$\dot{\hat{\phi}} = \dot{\phi}_{gyro} + k\left(\phi_{tilt\ sensor} - \hat{\phi}\right) \tag{4}$$

In the frequency domain, the relation between the estimated roll angle and the gyroscope roll rate and tilt angle sensor measured roll angle is as follows:

$$\hat{\phi} = \frac{1}{s+k}\dot{\phi}_{gyro} + \frac{k}{s+k}\phi_{tilt\ sensor} \tag{5}$$

Thus, the estimate combines the low frequency content of the angle estimate from the tilt sensor with the high frequency content of the integrated signal from the gyroscope. This helps eliminate the drift from integration of the gyroscope.

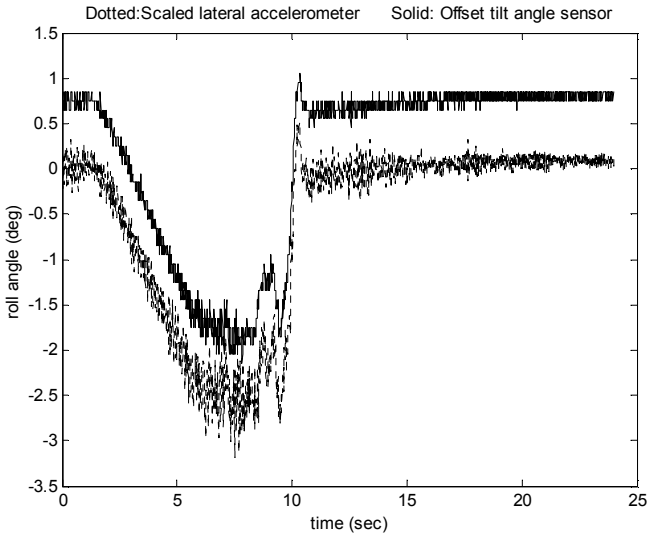


**Figure 3: Signals from tilt angle sensor and lateral accelerometer for swept steer experiment**

Figure 3 shows the signal from the tilt angle sensor for experiments conducted using a large SUV as a test vehicle. In this experiment, a swept steer angle was used with the vehicle operating at a longitudinal speed of 50 mph. It can be seen that the tilt angle sensor closely tracks the lateral accelerometer signal, after appropriate scaling. This is due to the fact that the angle calculation in the tilt sensor is based on the use of a lateral and a vertical accelerometer. The low frequency portion of the tilt angle signal is expected to be reliable.

Figure 4 shows a comparison of the roll rate, as measured by the gyroscope and as estimated from differentiation of the tilt angle sensor. It can be seen that the roll rate from differentiation of the tilt sensor lacks many of the transient features of the roll rate from the gyroscope. There is significant transient error in the tilt angle sensor, as shown by the circled portions of the curves in Figure 4.

Figure 5 shows the roll angle sensor as estimated by the kinematic algorithm of equation (4). It can be seen that the

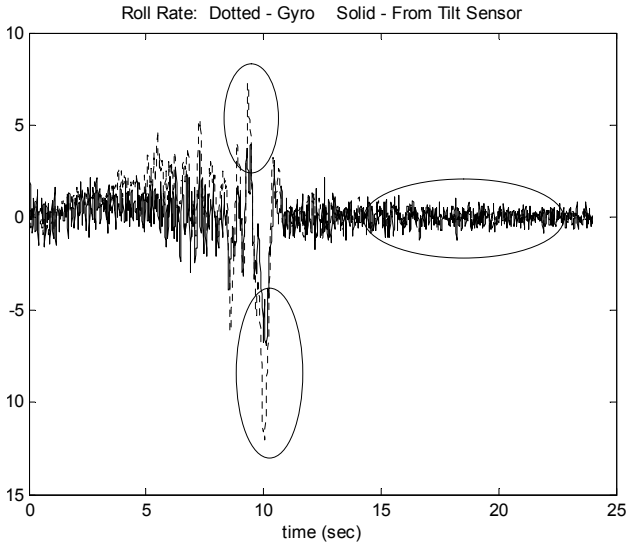


**Figure 4: Signals from gyroscope and differentiation of tilt angle sensor for swept steer**

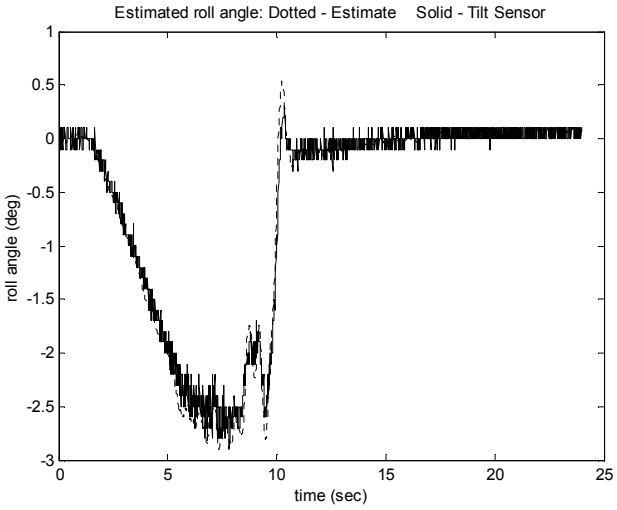


**Figure 5: Roll angle estimate from kinematic observer and tilt angle sensor**

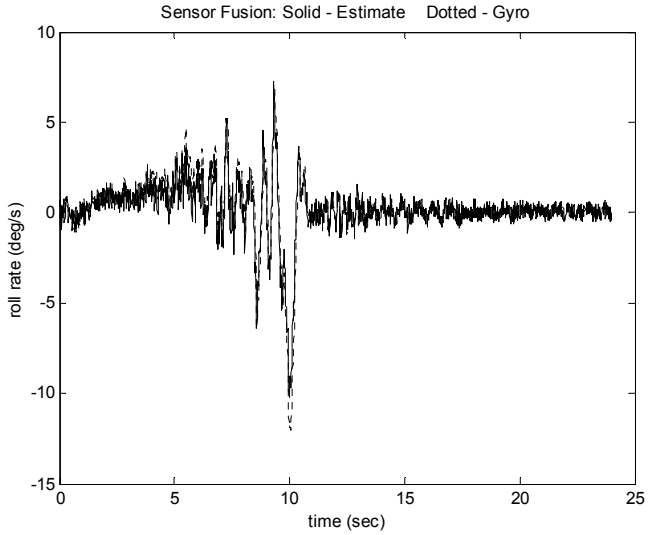


**Figure 6: Roll rate estimate from kinematic observer and gyroscope**

estimated roll angle tracks the steady state tilt angle signal, except for the better transient performance it provides during the period between 9 and 11 seconds. Figure 6 shows the roll rate as estimated by the kinematic algorithm and by the gyroscope. It can be seen that the roll rate estimate from the kinematic algorithm is a far better match for the gyroscope signal than the roll rate as estimated from differentiation of the tilt angle sensor, previously studied in Figure 4.

## 3. DYNAMIC OBSERVER

An alternate approach to estimation of roll angle is to use an observer based on a dynamic model of the vehicle roll dynamics, using only the lateral acceleration and a roll rate gyroscope as the measurements for the observer. Since a lateral accelerometer is anyway required for the rollover index calculation, the only additional sensor being used here then is the roll rate gyroscope. The need for the tilt angle sensor is eliminated.

To develop a dynamic model for the roll dynamics of the vehicle, consider the free body diagram in Figure 7.

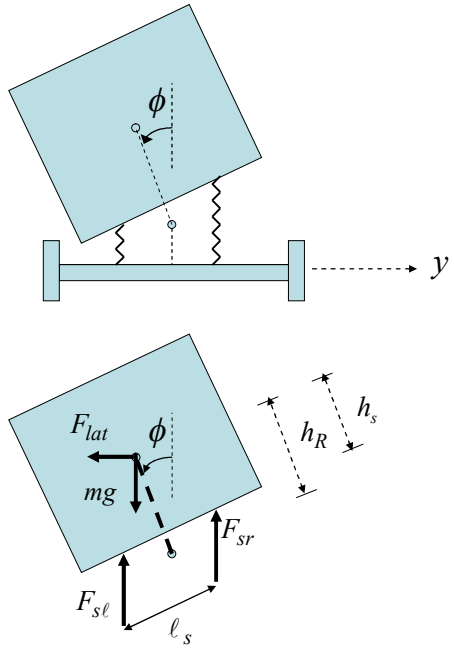


**Figure 7: Roll dynamics and free body diagram**

It should be noted that the d'Alembert's force $F_{lat}$ is applied at the c.g. of the vehicle. Vertical force yields the sum of the suspension forces as

$$F_{sl} + F_{sr} = mg \tag{6}$$

Taking moments about the roll center, the roll dynamics equation can be written as

$$\begin{aligned}(I_{xx} + mh_R{}^2)\ddot{\phi} &= \sum M_x \\ &= F_{lat}h_R\cos\phi + mgh_R\sin\phi \\ &\quad - F_{sl}\frac{\ell_s}{2}\cos\phi - F_{sl}(h_R - h_s)\sin\phi \\ &\quad + F_{sr}\frac{\ell_s}{2}\cos\phi - F_{sr}(h_R - h_s)\sin\phi\end{aligned} \tag{7}$$

or

$$\left(I_{xx} + mh_R{}^2\right)\ddot{\phi} = F_{lat}h_R\cos\phi + mgh_R\sin\phi + \frac{\ell_s}{2}\cos\phi\left(F_{sr} - F_{sl}\right) - \left(F_{sl} + F_{sr}\right)(h_R - h_s)\sin\phi \quad (8)$$

The suspension forces $F_{sl}$ and $F_{sr}$ act on both sides of the suspension springs (Figure 8). The suspension deflections on the left side and the right side due to roll are as follows:

$$z_{s\ell} = \frac{\ell_s}{2}\sin\phi + \left(h_R - h_s\right)(\cos\phi - 1) \text{ and}$$

$$z_{s\ell} = -\frac{\ell_s}{2}\sin\phi - \left(h_R - h_s\right)(\cos\phi - 1)$$

Hence, the suspension forces are

$$F_{sl} = \frac{mg}{2} + k\frac{\ell_s}{2}\sin(\phi) + k(h_R - h_s)(\cos\phi - 1) \quad (9)$$

$$F_{sr} = \frac{mg}{2} - k\frac{\ell_s}{2}\sin(\phi) - k(h_R - h_s)(\cos\phi - 1) \quad (10)$$

If we assume, $h_R \approx h_s$, this yields

$$F_{sl} - F_{sr} = k\ell_s\sin\phi \quad (11)$$

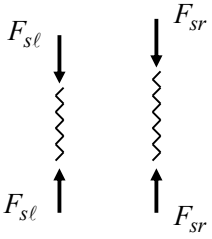


**Figure 8: Suspension forces**

Substituting from equations (11) and (6) into (8)

$$\left(I_{xx} + mh_R{}^2\right)\ddot{\phi} = F_{lat}h_R\cos\phi + mg\,h_R\sin\phi - \frac{1}{2}k\ell_s{}^2\cos\phi\sin\phi \quad (12)$$

Including suspension damping in addition to stiffness, the roll dynamics can finally be written down as

$$\left(I_{xx} + mh_R{}^2\right)\ddot{\phi} = ma_y h_R\cos\phi + mg\,h_R\sin\phi - \frac{1}{2}k\ell_s{}^2\cos\phi\sin\phi - \frac{1}{2}c\ell_s{}^2(\cos^2\phi)\dot{\phi} \quad (13)$$

It should be noted that the roll dynamics depend on the lateral dynamics through the lateral acceleration term $a_y$. By avoiding further expansion of this term in terms of lateral tire forces and lateral dynamic states, a complicated coupled set of equations between roll and lateral dynamics is avoided. Instead, the variable $a_y$ is assumed to be measured.

The following observer is proposed for estimation of roll angle:

$$\dot{\hat{\phi}} = \dot{\phi}_{meas} + k\left(\hat{\phi}_{\ell f} - \hat{\phi}\right) \quad (14)$$

$$\left(I_{xx} + mh_R{}^2\right)\ddot{\hat{\phi}}_{\ell f} = ma_y h_R\cos\phi_{\ell f} + mgh_R\sin\phi_{\ell f} - \frac{k}{2}\ell_s{}^2\sin\phi_{\ell f} - \frac{c}{2}\left(\ell_s{}^2\cos\phi_{\ell f}\right)\dot{\phi}_{\ell f} \quad (15)$$

The first equation in the observer combines the low frequency roll angle estimate with integrated roll rate from the gyroscope. The second equation is a replica of the roll dynamics model. Define the estimation error

$$\tilde{\phi} = \phi - \phi_{\ell f} \quad (16)$$

Subtracting equation (15) from equation (13)

$$\left(I_{xx} + mh_R{}^2\right)\ddot{\tilde{\phi}} = ma_y h_R(\cos\phi - \cos\phi_{\ell f}) + mg\,h_s(\sin\phi - \sin\phi_{\ell f}) - \frac{1}{2}k\ell_s{}^2(\cos\phi\sin\phi - \cos\phi_{\ell f}\sin\phi_{\ell f}) - \frac{1}{2}c\ell_s{}^2\left[(\cos^2\phi)\dot{\phi} - \cos^2\phi_{\ell f}\dot{\phi}_{\ell f}\right] \quad (17)$$

It can be shown that the estimation error dynamics in equation (17) are globally asymptotically stable for zero lateral acceleration. Furthermore, the error dynamics are locally asymptotically stable for non-zero bounded lateral acceleration.

It should be noted that use of the observer in equations (14) and (15) requires knowledge of the roll inertia, height of c.g. and suspension spring stiffness. Knowledge of the damping coefficient is not important, since it only affects the transient performance of the observer. The transient performance can be corrected from fusion with the gyroscope signal, as in equation (15).

## 4. EXPERIMENTAL RESULTS

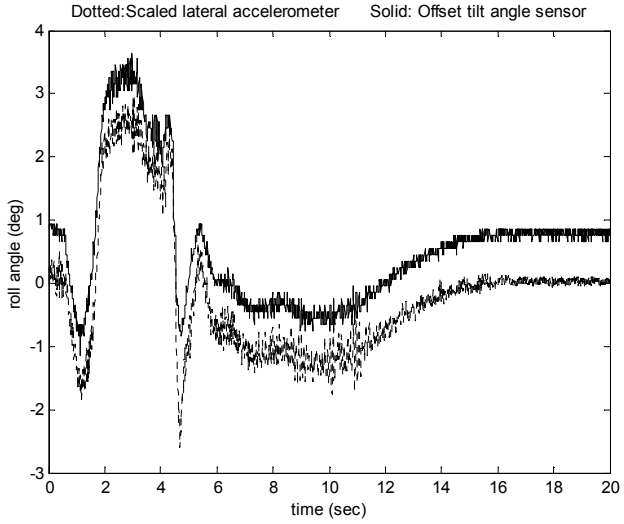


**Figure 9: Tilt angle sensor and accelerometer signals for FMVSS Data**

Figure 9 shows the tilt angle sensor signal for steering consisting of a sine with dwell maneuver. Again it can be seen that the tilt angle sensor signal closely tracks the lateral accelerometer signal. However, as shown in Figure 10, the differentiated tilt sensor signal has significant transient error

compared to the roll rate signal as measured by the gyroscope.

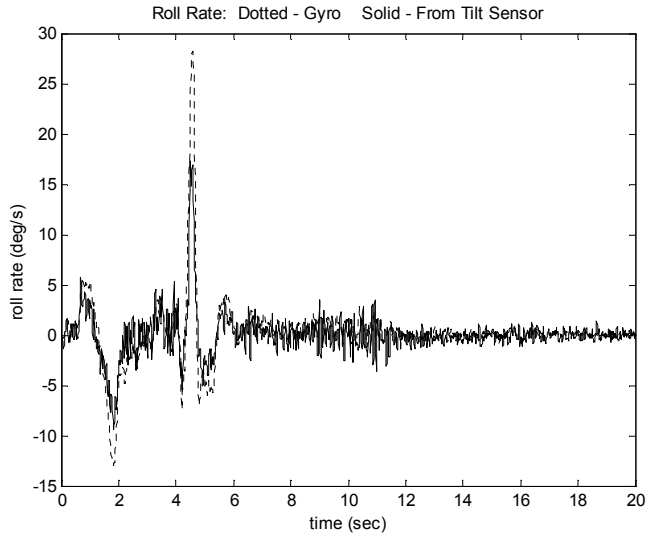


**Figure 10: Roll rate from gyroscope and differentiation of tilt angle signal for FMVSS Data**

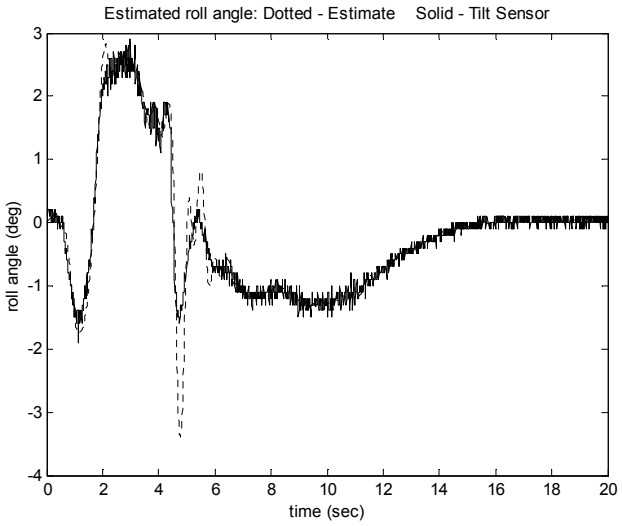


**Figure 11: Roll angle estimated from dynamic observer**

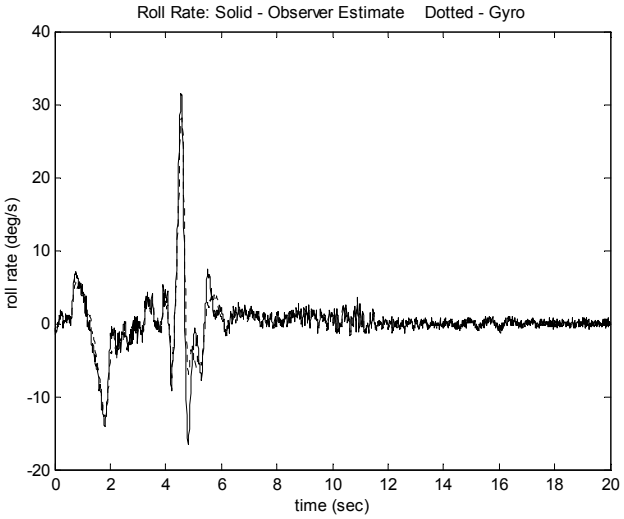


**Figure 12: Roll rate estimated from dynamic observer**

Figure 11 shows the estimated roll angle using the dynamic observer of equations (14) and (15). It can be seen that the roll angle tracks the steady state values of the tilt angle sensor but has significantly richer transient features in its signal, seen especially in the time duration between 4 and 7 seconds in the shown plot.

Figure 12 shows the estimated roll rate from the dynamic observer. It can be seen that the estimated roll rate matches the roll rate signal from the gyroscope much better than the differentiated tilt angle signal.

## 5. C.G. HEIGHT ESTIMATION

As described in section 1, the height of the c.g. of the vehicle plays an important role in the rollover index. The c.g. height can change significantly in SUVs, military vehicles (due to top loading) and trucks. Furthermore, there is no convenient method available to measure c.g. height. Unlike longitudinal c.g. position which can be obtained by measuring weights at the front axle and rear axle at a weigh station, there is no convenient technique for measuring c.g. height.

This section proposes and experimentally evaluates an algorithm for c.g. height estimation. Start with the following model for the roll dynamics of the vehicle

$$\left(I_{xx} + mh_R{}^2\right)\ddot{\phi} = ma_y h_R \cos\phi + mg\, h_s \sin\phi - \frac{1}{2}k\ell_s{}^2 \cos\phi \sin\phi - \frac{1}{2}c\ell_s{}^2(\cos^2\phi)\dot{\phi} \quad (18)$$

At steady state conditions (during steady cornering), the roll rate and acceleration can be assumed to be constant. In that case, equation (18) becomes

$$0 = ma_y h_R \cos\phi + mg\, h_s \sin\phi - \frac{1}{2}k\ell_s{}^2 \cos\phi \sin\phi \quad (19)$$

The height of the c.g. $h_R$ can then be obtained as

$$h_R = \frac{\frac{k}{2}\ell_s{}^2 \cos\phi \sin\phi}{ma_y \cos\phi + mg \sin\phi} \quad (20)$$

Equation (20) can be used to find the height of the c.g. in real-time. Two important issues, however, need to be noted:

1) The derivation of this equation assumes steady state cornering in which the roll angle is constant. Hence it will lead to errors during time periods when the roll rate and roll acceleration are non zero.
2) The equation requires that the roll angle be non zero. In the case where the roll angle is zero, as when the car is being driven straight with zero steering, both the numerator and denominator in equation (20) are zero.

Hence, in order to apply this technique for c.g. height estimation, it is required that the data used be from a maneuver in which the vehicle is under a steady cornering maneuver with non-zero steering. Techniques such as fuzzy logic based methods or others can be used to extract portions

of data during driving which constitute steady state cornering. Since c.g. height is a quasi-constant parameter and does not change for long periods of time, this is a viable approach.

Figure 13 shows the estimated c.g. height for a constant steering angle maneuver on the same experimental vehicle as described earlier. The time window between 10 and 20 seconds was chosen as being appropriate for use towards steady state cornering data. It can be seen that the c.g. height is estimated to be approximately around 0.9 meters. The use of a low-pass filter can smooth out the raw signal shown in the figure and yield a relatively constant c.g. height estimate.

Figure 14 shows the estimated c.g height for a swept steering maneuver in which the steering angel continuously increases and then briefly remains a constant. It can be seen that the c.g. height estimate varies during the increasing steering angle (shown by increasing lateral acceleration), but eventually settles down to an estimate of around 0.9 meters.

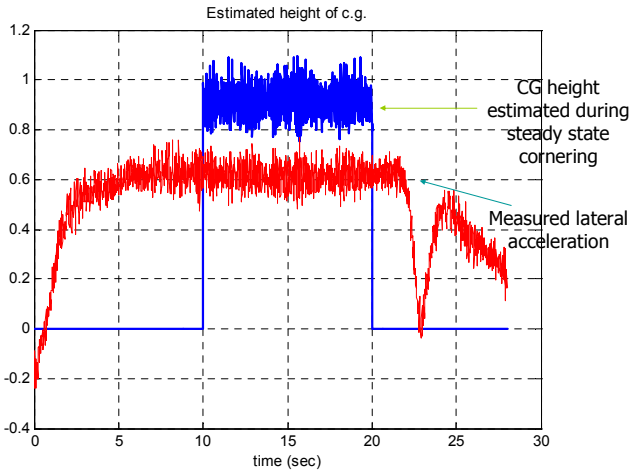


**Figure 13: Estimated c.g. height for steady state steering**

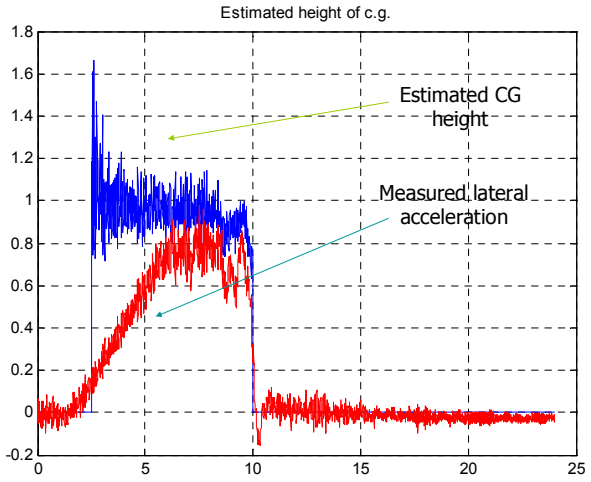


**Figure 14: Estimated c.g. height for swept steering**

## 6. CONCLUSIONS

Roll angle and height of the center of gravity are important variables that play a critical role in the calculation of real-time rollover index for a vehicle. Sensors to measure roll angle are expensive. Sensors to estimate the c.g. height of a vehicle do not exist.

This paper focused on algorithms to estimate real-time roll angle and c.g. height. The algorithms investigated include a sensor fusion algorithm that utilizes a low frequency tilt angle sensor and a gyroscope and a dynamic observer that utilizes only a lateral accelerometer and a gyroscope. The performance of the developed algorithms was investigated using experimental tests on a large SUV. Experimental data confirm that the developed algorithms performed reliably in a number of different maneuvers that include constant steering, ramp steering, and sine with dwell steering tests. The results in the paper provide solutions that will enable accurate calculation of rollover index, thus enabling better rollover prevention systems to be developed.

## References


[1] B. Chen and H. Peng, "Differential braking based rollover prevention for for sport utility vehicles with human-in-the-loop evaluations," Vehicle System Dyanmics, Vol. 36, No. 4-5, pp. 359-389, 2001.

[2] C.R. Carlson and J.C. Gerdes, "Optimal Rollover Prevention with Steer by Wire and Differential Braking," ASME International Mechanical Engineering Congress and Exposition, pp. 345-355, November, 2003.

[3] G.J. Forkenbrock, W.R. Garrott, M. Heitz and B.C. O'Harra, "Experimental Examination of J-Turn and Fishhook Maneuver that may Induce On-Road Untripped Light Vehicle Rollover," SAE Paper No. 2003-01-1008, 2003.

[4] A. Hac, T. Brown and J. Martens, "Detection of Vehicle Rollover," SAE Technical Paper Series, 2004-01-1757, SAE World Congress, 2004.

[5] J.Y. Lew, D. Piyabongkarn, and J.A. Grogg, "Minimizing Dynamic Rollover Propensity with Electronic Limited Slip Differentials," *SAE Transactions Journal of Passenger Cars: Mechanical Systems*, pp. 1183-1190, SAE book number V115-6, 2006.

[6] E.K. Liebemann, K. Meder, J. Schuh and G. Nenninger, "Safety and Performance Enhancement: The Bosch Electronic Stability Control (ESP)," *SAE Paper* No. 2004-21-0060.

[7] P.J. Liu, S. Rakheja and A.K.W. Ahmed, "Detection of Dynamic Roll Instability of Heavy vehicles for Open-Loop Rollover Control," SAE Paper No. 973263.

[8] NHTSA, USDOT. 2003 Fatality Analysis Reporting System (FARS). http://www-fars.nhtsa.dot.gov/Main/index.aspx.

[9] D. Odenthal, T. Bunte and J. Acjermann, "Nonlinear Steering and Braking Control for Vehicle Rollover Avoidance," Proceedings of the European Control Conference, 1999.

[10] D. Piyabongkarn, R. Rajamani, J. Grogg and J. Lew, "Development and Experimental Evaluation of a Slip Angle Estimator for Vehicle Stability Control," *IEEE Transactions on Control Systems Technology,* Vol. 17, No. 1, pp. 78-88, January 2009.

[11] S. Takano and Nagai, M., "Dynamic Control of Large Vehicles for Rollover Prevention," pp. 85-89, IEEE IVEC, 2001.

[12] H.E. Tseng, B. Ashrafi, D. Madau, T.A. Brown, and D. Recker, "The Development of Vehicle Stability Control at Ford," *IEEE/ASME Transactions on Mechatronics*, Vol. 4, No. 3, pp. 223-234, Sep. 1999.

[13] K. Yi, J. Yoon, and D. Kim, "Model-Based Estimation of Vehicle Roll State for Detection of Impending Vehicle Rollover," *Proceeding of the American Control Conference*, pp. 1624-1629, New York, July 11-13, 2007.

[14] J. Yoon, D. Kim and K. Yi, "Design of a Rollover Index Based Vehicle Stability Control Scheme," Vehicle System Dynamics, Vol. 45, No. 5, pp. 459-475, May 2007.